Fabrication of a polymer-based torsional vertical comb drive using a double-side partial exposure method

2008 J. Micromech. Microeng. 18 035014

(http://iopscience.iop.org/0960-1317/18/3/035014)

J. Micromech. Microeng. **18** (2008) 035014 (7pp) doi:10.1088/0960-1317/18/3/035014

Fabrication of a polymer-based torsional vertical comb drive using a double-side partial exposure method

Junwei Chung and Wensyang Hsu

Department of Mechanical Engineering, National Chiao Tung University, 1001 Ta Hsueh Road, Hsinchu, Taiwan

E-mail: whsu@mail.nctu.edu.tw

Received 16 July 2007, in final form 2 January 2008
Published 24 January 2008
Online at stacks.iop.org/JMM/18/035014

Abstract

A novel approach which uses a double-side partial exposure method to fabricate a polymer-based torsional vertical comb drive (VCD) with thick photoresist AZ9260® as the structural material is proposed in this paper. Front-side partial exposure defines the height of the fixed lower fingers, and back-side partial exposure creates the suspending space of the upper fingers, where the overlap and self-alignment between fingers can easily be achieved in this way. It does not need any sacrificial layer and etching process. A metal layer is finally deposited on the structural surface by a sputtering system for suitable electric conductivity to activate the polymer torsional VCD. The finite element method is used here to simulate the capacitance at different finger positions, and twelfth-order polynomial curve fitting is performed to obtain capacitance as a function of finger displacement. Then the rotation angle can be calculated analytically with the capacitance function. Also, the static deflection and dynamic response of polymer torsional VCDs are characterized experimentally, where the dimensions of the torsion plate are 300 μm wide and 360 μm long with movable fingers of length 100 μm; the torsion spring is 60 μm long and 4 μm wide. Both have a thickness of 31 μm, and the initial overlap is 11 μm in depth and 80 μm in length between the lower and upper fingers. By comparing the simulated and experimental results, the feasibility of the proposed fabrication method of polymer torsional VCDs is verified with a measured rotation angle of 2.31° under a driving voltage of 158.3 V.

(Some figures in this article are in colour only in the electronic version)

1. Introduction

As a well-known component, the electrostatic comb drive has rapidly occupied an important position in micro electromechanical system (MEMS) technology since the first report by Tang *et al* [1]. With two sets of fingers, the comb drive provides constant output force and good linearity on capacitive sensing over a considerable displacement range because of the constant gap between the stationary finger and movable finger during the operation. Therefore, the comb drive has been widely investigated, such as the optimal shape design [2] and the sub-micron gap comb drive [3], and employed for MEMS applications, such as filters [4], accelerometers [5], gyroscopes [6] and optical switches [7].

In addition to operation in the in-plane direction, a comb drive has also been fabricated with two sets of fingers owing a vertical offset to cause out-of-plane motion, which is called the vertical comb drive (VCD). Compared to the parallel plate electrostatic actuator, the VCD ideally generates a steady force over its entire stroke under one applied voltage, and exhibits no pull-in effect. Therefore, VCDs are suitable for applications requiring large out-of-plane displacement, low driving voltage, low power consumption and high operation speed. For these superior characteristics, many investigations on the VCDs have been reported in recent years [8–19]. In this literature, the fabrication methods could be divided into two categories. The first approach fabricated two sets of fingers owing a natural offset, such as the SUMMiT-V process [8], polysilicon

refilled and bulk etching [9], the bonding method [10], the SOI-based technique combining DRIE etching [11–13], multiple DRIE etching on a single-crystal silicon substrate [14] and micromachining on a (1 1 1) single-crystal silicon substrate [15, 16]. The second approach used the deforming mechanism to elevate or degrade one set of the comb fingers to create the required initial offset, such as the bending beam caused by residual stress [17], photoresist reflowing [18] and plastic deformation [19]. All these above-mentioned methods used single-crystal silicon or polysilicon as the structural materials.

In contrast to silicon-based materials, polymers have become another attractive material in the MEMS technology recently because of their relatively low cost and much easier processing steps. For example, polycarbonate (PC) and polymethylmetacrylate (PMMA) have been utilized to fabricate high aspect ratio microstructures by a hot embossing method for MEMS applications [20]. Micro fluidic devices for micro total analysis system (μ-TAS) applications were also widely fabricated by PMMA, PC, polypropylene (PP) and polydimethylsiloxane (PDMS), etc [21–23]. In addition to passive components, active micro devices have also been demonstrated by polymer materials to lower the cost, such as the electrostatic comb drive constructed by PMMA via the hot embossing technique [24], or by the thick negative photoresist SU-8 [25]. An accelerometer has also been fabricated using SU-8 as the structural material [26], and polymer micromechanical devices coated with a metal layer via the electroless deposition technique have also been demonstrated [27]. Therefore, polymers are becoming a greatly important low-cost alternative to their silicon- or glass-based counterparts. However, no vertical comb drive made of polymer material has been reported yet.

In this paper, a novel approach to fabricating a polymer torsional vertical comb drive is proposed. Without any additional sacrificial layer, the proposed double-side partial exposure method is applied to the positive thick photoresist AZ9260® to carve out the suspending upper fingers and the fixed lower fingers. With a proper overhang design to realize electric isolation, the metal layer deposited on the structural surface by sputtering provides suitable electric conductivity. This approach provides a simple, flexible and low-cost solution to fabricate polymer VCDs.

2. Operation and analysis

As the schematic illustration in figure 1 shows, the torsional vertical comb drive (VCD) demonstrated in this paper consists of two sets of comb fingers. One set of fingers is fixed on the substrate, and the other set of fingers is suspended and connected to a suspending plate which is supported by anchors through torsion springs. With the voltage applied between the upper and lower fingers, the VCD could be driven into torsional motion by the electrostatic force until it is balanced by the mechanical force of the torsion springs. By solving the force balance equation, the relationship between the driving voltage and torsion angle could be determined.

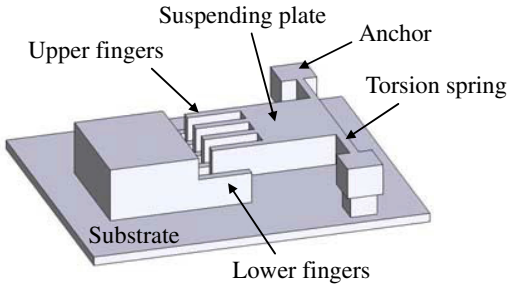

Figure 1. A schematic illustration of the torsional vertical comb drive.

2.1. Electrostatic force

In general, the electrostatic force per unit length generated by the comb drive with one finger pair is given by

$$F_e(z) = \frac{1}{2}\frac{\mathrm{d}C}{\mathrm{d}z}V^2 \tag{1}$$

where C is the capacitance per unit length between a single pair of fingers, z is the vertical displacement in the out-of-plane direction and V is the applied voltage. However, the capacitance C could not be considered as a simple parallel plate assumption with the fringing fields due to the limited height (or thickness) of fingers. To characterize the $\mathrm{d}C/\mathrm{d}z$ relationship, the finite element method (FEM) through software ANSYS is used to simulate the capacitance of single pair fingers at different displacements, z. Then, twelfth-order polynomial curve fitting is performed to obtain the capacitance C as a function of displacement, z, which is expressed as

$$C(z) = a_{12}z^{12} + a_{11}z^{11} + a_{10}z^{10} + \cdots + a_2z^2 + a_1z + a_0. \tag{2}$$

As illustrated in figure 2(a), in addition to the case without considering an electrically conductive substrate, the so-called bottom plate, the condition of lower fingers with a conductive bottom plate is also analyzed. Figure 2(b) shows one example of the simulation and fitting results with a finger height of 35 μm, a finger width of 14 μm and a gap of 4 μm. The fitting curve agrees well with the simulation data. For the fingers with a conductive bottom plate, the capacitance is similar to that without a conductive bottom plate at the initial 2/3rds of the stroke, but quite different in the final part of the stroke.

2.2. Force balance analysis

As illustrated in figure 3, the torque induced by the electrostatic force of the VCD could be expressed as

$$T_e = \int_{x1}^{x2} nF_e(z)L_r\,\mathrm{d}x \tag{3}$$

where n is the number of finger pairs, $x1$ and $x2$ indicate the overlap region of the upper and lower fingers along the suspending plate (x direction) and L_r is the moment arm of the electrostatic force of a single finger pair, $F_e(z)$, about the torsional axis and equating $x\cos\theta$, in which θ is the rotation

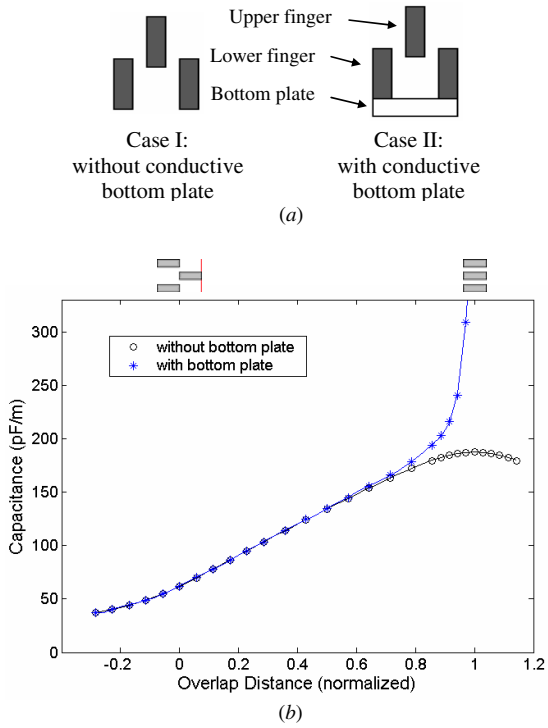

Figure 2. The simulated cases and results: (*a*) two simulated cases: with/without the conductive bottom plate; (*b*) the simulated capacitance of single pair fingers at different displacements z and the curve fitting results; the overlap distance is normalized by a finger height of 35 μm.

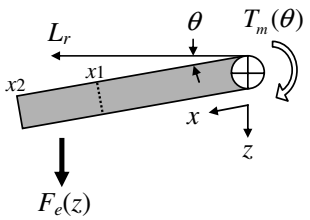

Figure 3. Illustration of the torque induced by electrostatic force, from a side view of the upper finger and suspending plate, where $T_m(\theta)$ is the torque induced by the mechanical force of the torsion springs.

angle of the VCD. Because the vertical displacement z could be expressed as $x \sin\theta$, equation (3) could be re-written as

$$T_e(\theta) = \frac{nV^2 \cos\theta}{2} \left[\sum_{k=1}^{12} \frac{k(a_k x^{k+1} \sin^{k-1}\theta)}{k+1} \right]_{x1}^{x2}. \quad (4)$$

Equation (4) describes the torque induced by the electrostatic force under different rotation angles for a given voltage. In addition, the torque generated by the mechanical force of the torsion springs could be described by

$$T_m(\theta) = -\frac{G\theta(b^3h + bh^3)}{6L} \quad (5)$$

where G is the shear modulus of elasticity, b, h and L are the width, height and length of the torsion springs, respectively. Using equations (4) and (5), the rotation angle of the VCD could be found.

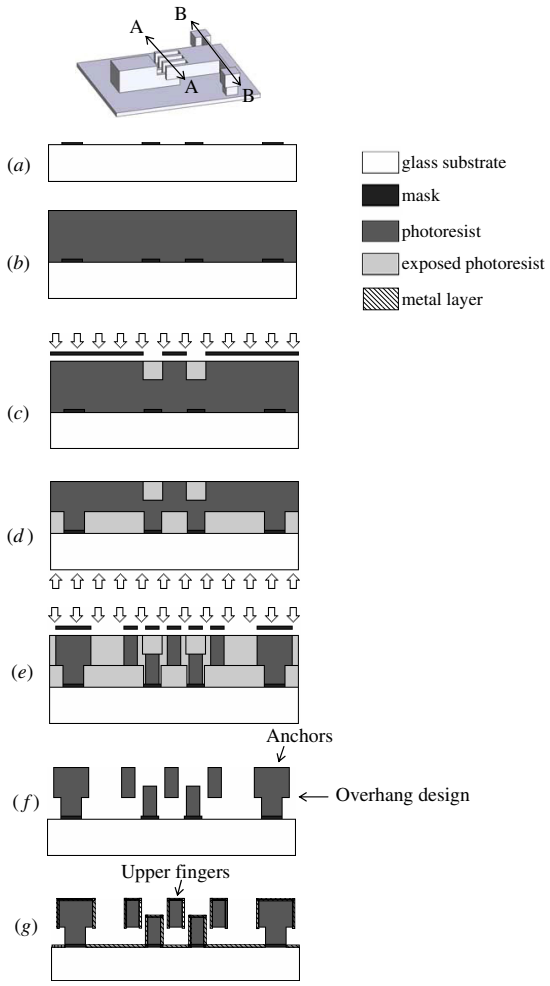

Figure 4. The fabrication process of the polymer torsional VCD on the AA cross-section for fingers, and BB cross-section for anchors; (*a*) defining the Ti film as the backside mask; (*b*) coating the thick positive photoresist; (*c*) the front-side partial exposure; (*d*) the backside partial exposure; (*e*) the full exposure to define the overall structure; (*f*) development and release with overhanging design on the anchors; (*g*) sputtering the Cu layer with electric isolation on the anchor.

3. Fabrication

For the positive photoresist, only photoresist suffering the exposure dosage over the threshold value will be removed during the development, so free-standing microstructures can be achieved by patterning the photoresist from the back side via dosage control. Here, a novel process using a partial exposure method in both front and back sides is employed to fabricate the polymer-based torsional vertical comb drive and needs only three masks in total.

Figure 4 shows the detailed fabrication procedure of the proposed polymer VCD. Soda-lime glass is used as the substrate, and the commercial positive thick photoresist AZ9260® (Clariant) is utilized to demonstrate this process. First, a Ti layer of 2500 Å is deposited and patterned by the lift-off process as the mask for the backside partial exposure, as shown in figure 4(*a*). Then, the photoresist AZ9260®

with a thickness of about 55 μm is spin-coated and soft-baked at 90 °C for 90 min, as shown in figure 4(*b*). After re-hydration, the photoresist is exposed by front-side partial exposure for the desired development depths, as shown in figure 4(*c*), which defines the height, i.e. thickness, of the lower fingers. Then, backside partial exposure is carried out for the suspending space of the upper fingers, as shown in figure 4(*d*), which provides the desired operation stroke of the VCD. Subsequently, full exposure is carried out to define the overall structure, as shown in figure 4(*e*), in which the upper and lower fingers are self-aligned to avoid the misalignment problem. After all the required exposing procedure, the final development is performed with the developer of AZ400k (20% diluted by de-ionized water). At this step, the release process of the VCD is also completed without any additional sacrificial layer and etching step. Then, the structure of the VCD is fabricated, as shown in figure 4(*f*), where the overhang design at the anchors is employed by defining a narrower width at the lower part of the anchors. Finally, in order to provide the desired electric conductivity to activate the VCD, a thin Cu layer with a thickness of 2000 Å is deposited on the structural surface by a sputtering system, and the overhang design can achieve electric isolation around the undercut of the anchors to avoid an electric short between the upper and lower sets of fingers, as shown in figure 4(*g*).

4. Experimental results and discussions

In this section, the parameters of photoresist processing are experimentally characterized, first for reliable fabrication of the vertical comb drive (VCD). Then, the fabrication results of polymer torsional VCDs by the proposed process are shown and discussed. Finally, the static and dynamic responses of the VCD are measured and compared with the simulation results.

4.1. Photoresist processing

In general, the development depth of photoresist is mainly controlled by the exposure dosage. In other words, a larger dosage creates a deeper depth. However, other processing parameters of photoresist, such as the development time and soft-bake time, also play important roles in this process. In addition to the increase of exposure dosage, longer development time will also enlarge the development depth of photoresist, but this enlargement could be evidently reduced by longer soft-bake time. Therefore, a proper set of parameters is needed to obtain stable fabrication results. Here, a photoresist thickness of about 55 μm, a soft-bake time of 90 min and a development time of 45 min are employed on the fabrication of polymer VCDs. With these parameters, figure 5 shows the development depths of AZ9260® under different exposure dosages. The results reveal that the development depth increases stably with the increasing exposure dosage. Depending on these experimental data, the desired suspending space of the upper fingers and the height of the lower fingers could be fabricated using the corresponding dosages.

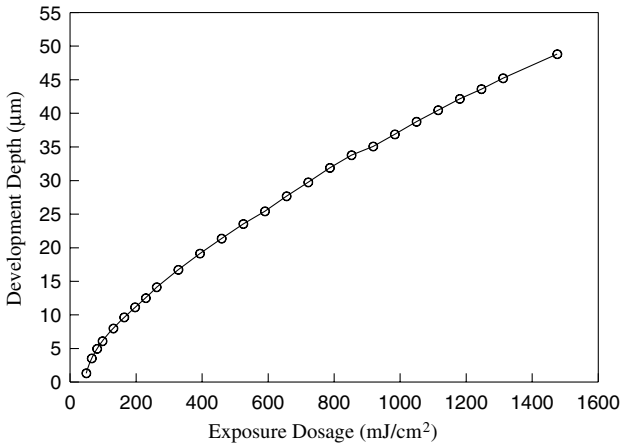

Figure 5. The relationship between the development depth and the exposure dosage of the photoresist AZ9260®.

4.2. Fabrication results

Under the photoresist processing conditions described above, polymer VCDs with two levels both in front and back sides are fabricated by the proposed process. Figure 6(*a*) shows the fabricated VCD made of AZ9260® after the final deposition of Cu by sputtering, where the size of the suspending plate is 300 μm wide and 360 μm long, and the width and length of torsion springs are 4 μm and 60 μm, respectively. A thinner or narrower torsion bar both can reduce the torsion spring constant for a larger torsion angle, but it may also cause the stiction, vertically or laterally. In order to have a thinner torsion bar, there can be two approaches: (1) decreasing the thickness of the suspended plate and the torsion bar simultaneously by increasing the backside partial exposure dosage, but it will lead to a smaller overlap area and larger gradient residual strains; (2) just reducing the thickness of the torsion bar by introducing an extra mask, however, which not only complicates the fabrication process, but also may a cause stress concentration problem at the interface between the suspended plate and the torsion bar due to different thicknesses. Therefore, a narrow torsion bar would be a more feasible approach than a thin torsion bar on reducing the torsion spring constant. However, the vertical and lateral stiction problem limits us to further reduce the width of the torsion spring.

An applied partial exposure dosage of 426 mJ cm^{-2} creates a development depth of about 20 μm in the front-side direction, which increases the height of the lower fingers to about 35 μm. By introducing a partial exposure dosage of 525 mJ cm^{-2} in the backside direction, a suspending space of the upper fingers of about 24 μm is obtained, which indicates that the overlap depth between the fixed and movable finger is 11 μm, and the thickness of suspended structures is about 31 μm. It is found that a higher exposure dosage will enlarge the trench width and limit the gap size. Figures 6(*b*) and (*c*) show the closed view and top view of the finger structures, respectively, where the finger is 100 μm long, the overlap length between the fixed and movable fingers is around 80 μm, the finger width is 10 μm and the gap is 8 μm which is the minimum gap size we can achieve. Finally, the supporting

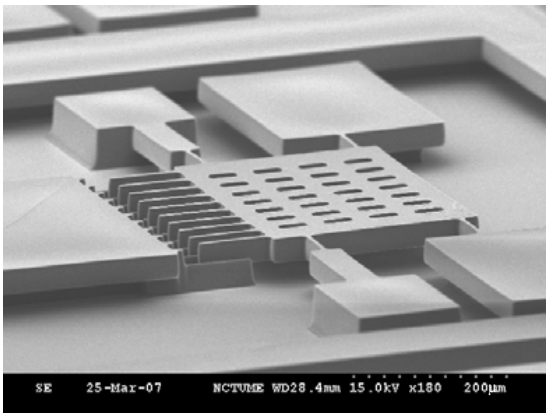

(*a*)

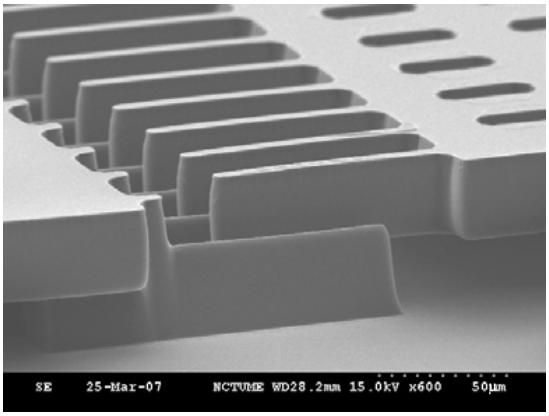

(*b*)

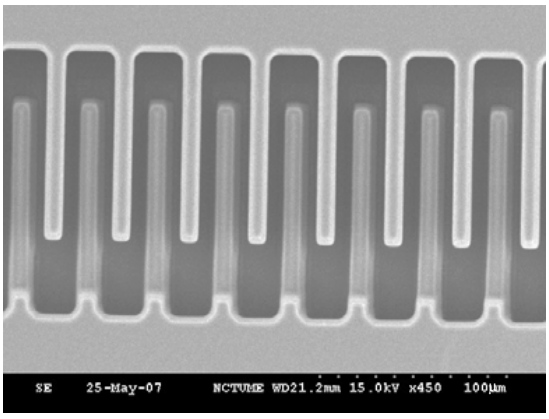

(*c*)

Figure 6. The fabricated polymer torsional vertical comb drive by the double-side partial exposure method; (*a*) over view of the VCD; (*b*) closed view and (*c*) top view of the finger structures.

bars near the upper fingers to avoid stiction are removed by the probe manually for the following measurements.

4.3. Measurement and comparison

The static deflection and dynamic responses of the polymer torsional VCD are measured in open air by a white light interferometer and a MEMS motion analyzer (MMA), respectively. In measuring the rotation angle, the surface

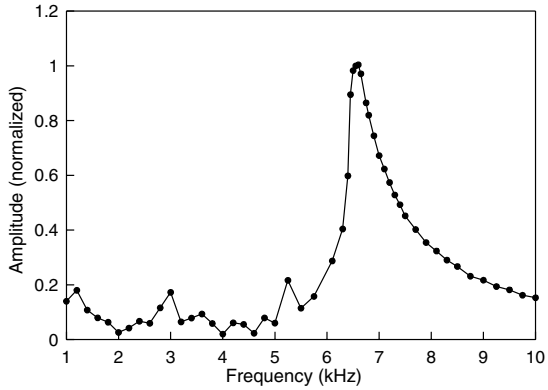

Figure 7. The dynamic response of the vertical comb drive; the peak response is obtained at 6.6 kHz.

profiles of the VCD in a steady state under different driving voltages are first determined by the white light interferometer. Then the rotation angle can be calculated by the relative deflection between two reference points, such as the movable finger tip and the torsion spring. For vibration measurement, a sinusoid wave is applied to the VCD with the frequency range from 1 KHz to 10 kHz, then the amplitude is recorded. By selecting the proper location, the dynamic responses at different frequencies can be obtained directly.

According to the measurement on static deflection, a maximum rotation angle of 2.31° can be achieved by a driving voltage of 158.3 V with the same designed dimensions as shown in figure 6 except that the gap size is 13 μm and the finger width is about 5 μm. Figure 7 shows the measured results of dynamic response, where the VCD is activated by a sinusoid wave with an amplitude of 20 V and an offset of 20 V, and the first-mode natural frequency of 6.6 kHz is obtained. With this characterized natural frequency, the elastic modulus could be found by further determining the density of photoresist. Here, a simple experiment is performed to obtain the density of AZ9260®. The photoresist is spin-coated on a wafer with the calibrated weight, and then patterned into a circle with a specified diameter. By determining the increase of total weight and the final thickness of the photoresist film, the density of photoresist could be obtained through the characterized value of weight over volume. Then, with the determined density of 1180 $\pm$ 7 Kg m^{-3} and first natural frequency of 6.6 kHz, an effective elastic modulus of 1.142 GPa is used in the FEM simulation, where Poisson's ratio is assumed to be 0.4. Figure 8 shows the simulated results of modal analysis, in which the model of the VCD includes the suspending plate, the torsion springs and the upper fingers. The second, third and fourth natural frequencies are also found to be 41.40 kHz, 44.10 kHz and 54.02 kHz, respectively.

With the above material properties, the static deflection of the polymer VCD is calculated by Matlab software through the analytical model described in section 2. Figure 9 shows the experimental and analytical results of the polymer torsional VCD, where the latter includes the cases with and without considering the conductive bottom plate. In the analytical results, the case without bottom plate electrodes presents more

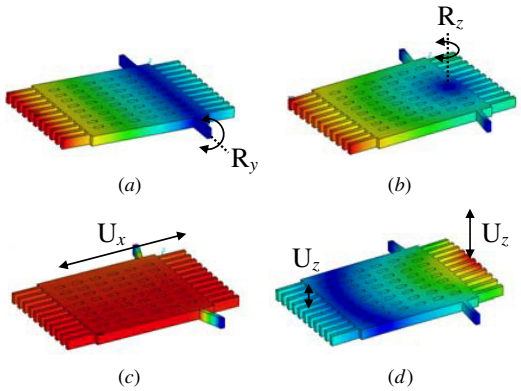

Figure 8. The mode shapes and natural frequencies of the vertical comb drive; (*a*) $f_1 = 6.60$ kHz, (*b*) $f_2 = 41.40$ kHz, (*c*) $f_3 = 44.10$ kHz, and (*d*) $f_4 = 54.02$ kHz.

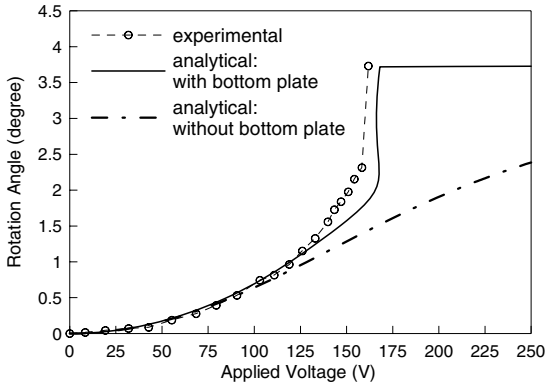

Figure 9. The experimental and analytical results of the static deflection of the vertical comb drive, where the analytical results include the cases with and without a conductive bottom plate.

linear behavior but a little smaller rotation angle under different driving voltages. For the case with a conductive bottom plate, a similar behavior is observed in the first half stroke but there is a pull-in effect at a rotation angle of 2.17° with an applied voltage of 167.37 V due to the obvious increase of the capacitance which induces the rapid rise of electrostatic force. By comparing to experimental results, where a snapping phenomenon is also observed between the voltages of 158.3 V and 161.8 V, the bottom plate effect has an evident influence on the performance of the VCD, especially at high driving voltage. Furthermore, according to our simulations, it is found that the metal layer on the upper finger bottom has little effect on the rotation angle, since the width of the upper finger, 5 μm, is much smaller than its height, 31 μm. For example, when the driving voltage is 160 V, the rotation angle will change only from 1.804° (metal layer on the upper finger bottom) to 1.792° (without a metal layer on the upper finger bottom).

The internal stress may also affect the performance of the torsional VCD. The residual gradient strain will result in a curved surface, which would lift the movable fingers up to have an extra offset and reduce the overlap area. However, the torsional VCD with a larger offset can provide a longer stroke to allow a larger rotation angle. In our case, the extra offset between the movable finger center and fixed finger center due to the internal stress is found to be around 3 μm initially, which is not considered in the simulation model. This might be the reason why experimental results show larger rotation angles around 150 V than simulation results. However, even the Young's modulus (1.142 GPa) of AZ9260 covered by a thin Cu layer is much lower than single crystal silicon (160–200 GPa); compared to torsional VCDs made of single crystal silicon reported previously [28, 29], the polymer torsional VCD fabricated here needs higher driving voltage to achieve the same rotation angle due to our limitations on fabrication capability. For example, the minimum gap size here is 8 μm, which could be further improved by a better exposure system. Another issue would the thickness of the polymer. A thicker photoresist will be helpful in providing a larger overlap area between fixed and movable fingers; also it may support a larger suspended space to avoid stiction without using supporting bars.

5. Conclusions

This investigation proposes a reliable approach to fabricating a polymer-based torsional vertical comb drive by using positive thick photoresist AZ9260® as the structural material. A double-side partial exposure method is employed to create the suspending upper fingers and the fixed lower fingers without any additional sacrificial layer and etching process. The proper processing parameters of photoresist for the fabrication of polymer torsional VCDs have been established. For the activation of the polymer VCDs, the metal layer deposited on the structural surface by a sputtering system provides the desired electric conductivity, while the overhang design realizes electric isolation. According to the measurement results, a rotation angle of 2.31° can be achieved by a driving voltage of 158.3 V, which agrees with the analytical results and verifies the feasibility of the proposed approach to fabricate polymer VCDs.

Acknowledgments

This work was partially supported by the National Science Council of the Republic of China under grant number NSC95–2218-E-009–023. The authors also would like to thank the staff at the Nano Facility Center of National Chiao Tung University for providing technical support.

References

[1] Tang W C, Nguyen T H and Howe R T 1998 Laterally driven polysilicon resonant microstructures *Tech. Dig. IEEE Micro Electro Mech. Syst. Workshop (Salt Lake City)* pp 53–9

[2] Ye W, Mukherjee S and MacDonald N C 1998 Optimal shape design of an electrostatic comb drive in microelectromechanical systems *J. Microelectromech. Syst.* **7** 16–26

[3] Hirano T, Furuhata T, Gabriel K J and Fujita H 1992 Design, fabrication, and operation of submicron gap comb-drive microactuators *J. Microelectromech. Syst.* **1** 52–9

[4] Lin L, Howe R T and Pisano A P 1998 Microelectromechanical filters for signal processing *J. Microelectromech. Syst.* **7** 286–94
[5] Park K Y, Lee W C, Jang H S, Oh Y S and Ha B J 1998 Capacitive sensing type surface micromachined silicon accelerometer with a stiffness tuning capability *Dig. IEEE/ASME MEMS Workshop (Heidelberg, Germany)* pp 637–42
[6] Tanaka K, Mochida Y, Sugimoto M, Moriya K, Hasegawa T, Atsuchi K and Ohwada K 1995 A micromachined vibrating gyroscope *Sensors Actuators* A **50** 111–5
[7] Juan W-H and Pang S W 1998 High-aspect-ratio Si vertical micromirror arrays for optical switching *J. Microelectromech. Syst.* **7** 207–13
[8] Hah D, Huang S T-Y, Tsai J-C, Toshiyoshi H and Wu M C 2004 Low-voltage, large-scan angle MEMS analog micromirror arrays with hidden vertical comb-drive actuators *J. Microelectromech. Syst.* **13** 279–89
[9] Selvakumar A and Najafi K 2003 Vertical comb array microactuators *J. Microelectromech. Syst.* **12** 440–9
[10] Lee J-H, Ko Y-C, Kong D-H, Kim J-M, Lee K B and Jeon D-Y 2002 Design and fabrication of scanning mirror for laser display *Sensors Actuators* A **96** 223–30
[11] Yeh J-L A, Jiang H and Tien N C 1999 Integrated polysilicon and DRIE bulk silicon micromachining for an electrostatic torsional actuator *J. Microelectromech. Syst.* **8** 456–65
[12] Hah D, Choi C-A, Kim C-K and Jun C-H 2004 A self-aligned vertical comb-drive actuator on an SOI wafer for a 2D scanning micromirror *J. Micromech. Microeng.* **14** 1148–56
[13] Milanović V 2004 Multilevel beam SOI-MEMS fabrication and applications *J. Microelectromech. Syst.* **13** 19–30
[14] Zhang Q X, Liu A Q, Li J and Yu A B 2005 Fabrication technique for microelectromechanical systems vertical comb-drive actuators on a monolithic silicon substrate *J. Vac. Sci. Technol.* B **23** 32–41
[15] Kim J, Park S and Cho D 2001 A novel electrostatic vertical actuator fabricated in one homogeneous silicon wafer using extended SBM technology *Transducers '01* pp 756–9
[16] Tsai J M-L, Chu H-Y, Hsieh J and Fang W 2004 The BELST II process for a silicon high-aspect-ratio micromaching vertical comb actuator and its applications *J. Micromech. Microeng.* **14** 235–41
[17] Jeong K-H and Lee L P 2005 A novel microfabrication of a self-aligned vertical comb drive on a single SOI wafer for optical MEMS applications *J. Micromech. Microeng.* **15** 277–81
[18] Hah D, Patterson P R, Nguyen H D, Toshiyoshi H and Wu M C 2004 Theory and experiments of angular vertical comb-drive actuators for scanning micromirrors *J. Sel. Top. Quantum Electron.* **10** 505–13
[19] Kim J, Choo H, Lin L and Muller R S 2003 Microfabricated torsional actuator using self-aligned plastic deformation *Transducers '03* pp 1015–8
[20] Becker H and Heim U 2000 Hot embossing as a method for the fabrication of polymer high aspect ratio structures *Sensors Actuators* A **83** 130–5
[21] Lee G-B, Chen S-H, Huang G-R, Sung W-C and Lin Y-H 2001 Microfabricated plastic chips by hot embossing methods and their applications for DNA separation and detection *Sensors Actuators* B **75** 142–8
[22] Becker H and Gärtner C 2000 Polymer microfabrication methods for microfluidic analytical applications *Electrophoresis* **21** 12–26
[23] Abgrall P 2007 Lab-on-chip technologies: making a microfluidic network and coupling it into a complete microsystem—a review *J. Micromech. Microeng.* **17** R15–49
[24] Zhao Y and Cui T 2003 Fabrication of high-aspect-ratio polymer-based electrostatic comb drives using the hot embossing technique *J. Micromech. Microeng.* **13** 430–5
[25] Dai W, Lian K and Wang W 2007 Design and fabrication of a SU-8 based electrostatic microactuator *Microsyst. Technol.* **13** 271–7
[26] Jeong S J and Wang W 2004 Microaccelerometers using cured SU-8 as structural material *Proc. SPIE* **5344** 115–23
[27] Eberhardt W, Gerhäußer Th, Giousouf M, Kück H, Mohr R and Warkentin D 2002 Innovative concept for the fabrication of micromechanical sensor and actuator devices using selectively metallized polymers *Sensors Actuators* A **97–98** 473–7
[28] Tsai J M-L, Chu H-Y, Hsieh J and Fang W 2004 The BELST II process for a silicon high-aspect-ratio micromaching vertical comb actuator and its applications *J. Micromech. Microeng.* **14** 235–41
[29] Jeong K-H and Lee L P 2005 A novel microfabrication of a self-aligned vertical comb drive on a single SOI wafer for optical MEMS applications *J. Micromech. Microeng* **15** 277–81